FILME SUBŢIRI CERAMICE DEPUSE PRIN CENTRIFUGARE CA ACOPERIRI PENTRU IMPLANTURI METALICE
CERAMIC THIN FILMS DEPOSITED BY SPIN COATING AS COATINGS FOR METALLIC IMPLANTS

CRISTINA BUSUIOC[1], IZABELA CONSTANTINOIU[1], MONICA ENCULESCU[2], MIHAELA BEREGOI[2], SORIN - ION JINGA[1]*

University Politehnica Bucharest, Str. G. Polizu nr. 1-6, cod 011061, Bucharest, Romania
[2] National Institute of Materials Physics,, 077125, Măgurele, Romania

Ceramic thin films belonging to SiO_2–P_2O_5–CaO–MgO–ZnO–CaF_2 system were obtained by combining the sol-gel approach with the spin coating technique. Titanium plates were employed as substrates. The deposited coatings were characterized in terms of composition, structure and morphology with the help of the following methods: X-ray diffraction, Fourier - transform infrared spectroscopy and scanning electron microscopy coupled with energy - dispersive X-ray spectroscopy. In order to assess the bioactivity of a potential metallic implant covered with such layers, the samples were immersed in simulated body fluid for 14 days and their surface was investigated. The results showed that the thin films calcined at a lower temperature have a better biological response due to the vitroceramic nature.

Au fost obţinute filme subţiri ceramice aparţinând sistemului SiO_2–P_2O_5–CaO–MgO–ZnO–CaF_2 prin combinarea abordării sol-gel cu tehnica depunerii prin centifugare. Ca substraturi au fost folosite plăcuţe de titan. Acoperirile depuse au fost caracterizate în ceea ce priveşte compoziţia, structura şi morfologia cu ajutorul următoarelor metode: difracţie de raze X, spectroscopie în infraroşu cu transformată Fourier şi microscopie electronică cu baleiaj cuplată cu spectroscopie de raze X cu dispersie după energie. Pentru a evalua bioactivitatea unui potenţial implant metalic acoperit cu astfel se straturi, probele au fost imersate în fluid biologic simulat timp de 14 zile şi a fost investigată suprafaţa lor. Rezultatele au arătat că filmele subţiri calcinate la o temperatură mai mică au un răspuns biologic mai bun datorită naturii vitroceramice.

Keywords: Ceramics; Thin films; Sol-gel; Spin coating; Medical implants.

1. Introduction

The hard tissues of human body often require replacement with artificial substitutes after the occurrence of accidents or diseases. Metallic implants, the first and most used materials for this purpose, present major weaknesses despite the suitable mechanical properties [1, 2]. These are related to corrosion [3], toxicity [4] and osseointegration [5]. In order to overcome the mentioned disadvantages, different types of materials, inorganic [6], organic [7] or hybrid [8], were deposited in the form of coatings on pure metals or alloys, the biological response being significantly improved. In other words, the solution to cancel the inherent bioinertia of metals consist in the growth of bioactive films on their surface [9], with the assurance of an optimal adhesion between the two phases. The category of inorganic layers has been widely studied due to the compositional resemblance to the natural bone. Glasses [6], ceramics[10] and glass-ceramics [11, 12] can be

included in the researchers' concerns regarding hard tissue engineering.

The employed synthesis methods have a great influence on the final properties of a material. Thus, the sol-gel method seems to be one of the most recommended, since it ensures purity through the high quality precursors, provides homogeneity at atomic scale and conserves the selected stoechiometry [13, 14]. It is a wet chemistry approach for the preparation of oxide materials based on the transition from sol to gel by means of the hydrolysis, condensation and polymerization [15].

On another hand, the fabrication of materials in the form of two-dimensional structures is an objective that can be attained by different techniques, such as: pulsed laser deposition [11, 12], magnetron sputtering [16], spin coating [17, 18] etc. The last one represents a cheap and fast way for producing thin or thick films by starting from a precursor solution that is applied on a rotating substrate. The process can be divided in four

steps, as follows: deposition, when a volume of precursor solution is laid on the surface of a suitable substrate; acceleration, when the liquid is spread towards the substrate edges by centrifugal force; flow, when the liquid drains radially outward and the excess leaves the surface as droplets; and evaporation, when the solvent volatilizes and the final thickness of the film is reached [19]. Among the parameters that control the thickness of an individual layer, can be mentioned: solution concentration, solution volume, acceleration, rotation speed, solvent type, number of layers etc.

Our research group previously published on the synthesis and characterization of vitroceramic thin films processed by the sol-gel technology and laser ablation, the findings being innovative and of genuine interest for the scientific community [11, 12]. As a consequence, the next step is to explore other compositions or processing conditions within the same system or to approach other related systems. Thus, MgO was integrated in the primary composition, the positive effects that it has on material behaviour in biological environment being well-known [20, 21]. This work reports on the synthesis of ceramic thin films belonging to a novel oxide system through a combined method, sol-gel coupled with spin coating, as well as on the implications of the processing parameters on the composition, morphology and bioactivity of the final coatings.

2. Experimental

Considering SiO_2–P_2O_5–CaO–MgO–ZnO–CaF_2 system, the following molar composition was selected: 38 % SiO_2, 4 % P_2O_5, 35.25 % CaO, 18 % MgO, 4 % ZnO and 0.75 % CaF_2. Tetraethyl orthosilicate ($Si(OC_2H_5)_4$, TEOS; 98 %, Aldrich), triethyl phosphate ($PO(OC_2H_5)_3$, TEP; ≥ 99 %, Merck), calcium nitrate tetrahydrate ($Ca(NO_3)_2 \cdot 4H_2O$; 99-102 %, Merck), magnesium nitrate hexahydrate ($Mg(NO_3)_2 \cdot 6H_2O$; 99-102 %, Merck), zinc nitrate hexahydrate ($Zn(NO_3)_2 \cdot 6H_2O$; 98 %, Sigma-Aldrich) and calcium fluoride (CaF_2; 99.9 %, Sigma-Aldrich) were used as sources of cations. A simple sol-gel procedure was followed in order to achieve a precursor solution containing all the desired species in the selected proportions. First, the alkoxides (1.43 mL TEOS and 0.23 mL TEP) were hydrolyzed separately, resulting in two clear solutions. Second, CaF_2 powder (0.0099 g)

was added to the first solution, while the water solubilized nitrates (1.4020 g $Ca(NO_3)_2 \cdot 4H_2O$, 0.7774 g $Mg(NO_3)_2 \cdot 6H_2O$ and 0.2004 g $Zn(NO_3)_2 \cdot 6H_2O$) to the second solution. Finally, the two solutions were mixed and strongly homogenized in order to obtain an opalescent solution for deposition (16.5 mL). The next step was to load the solution in a plastic syringe (5 mL) with a blunt tipped stainless needle (0.8 mm interior diameter) and to deposit four films on titanium substrates by spin coating, according to the parameters described in Table 1. The acceleration and period at maximum rotation speed were constant for all films, namely 1,000 rot/s and 5 min. The as-deposited coatings were thermally treated in order to remove the gas generating part and promote the crystallization process. The calcination was performed at the maximum temperature for 2 h, with a heating rate of 1 °C/min and natural cooling.

Basically, the films were synthesized by associating the sol-gel wet chemistry method with the spin coating deposition technique. The most important aspect is to perform the depositions before the sol is transformed into gel because the viscosity of a gel would not ensure appropriate conditions for the obtaining of uniform layers.

Part of the precursor solution until the gel formation for 12 h, whereupon gel was aged for 24 h and subsequently dried at 80 °C for other 24 h. The calcination temperature was selected after performing a thermal analysis on the dried gel with a Shimadzu DTG-60 equipment, in the 27 - 1000 °C temperature range. The crystalline features of the calcined samples were analyzed by X-ray diffraction (XRD), using a Shimadzu XRD 6000 diffractometer with Ni filtered Cu Kα radiation (λ = 0.154 nm), 2θ ranging between 5 and 80 °. The morphology and elemental composition of the films were determined through scanning electron microscopy (SEM) coupled with energy-dispersive X-ray spectroscopy (EDX), employing a FEI Quanta Inspect F scanning electron microscope. The biological behaviour of the coatings was assessed through an in vitro test, simulated body fluid (SBF) soaking for 14 days at 37 °C; the testing solution was obtained according to Kokubo et al. [22].

3. Results and discussion

The thermal analysis of the dried gel (Fig. 1)

Table 1

Processing parameters for the synthesis of thin films.
Parametrii de procesare pentru sinteza filmelor subţiri.

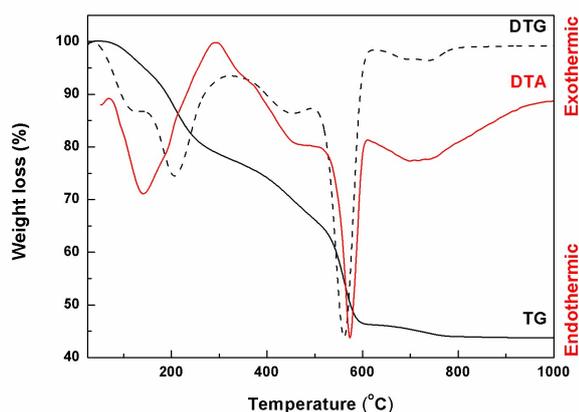| Sample name	Solution volume (drops)	Rotation speed (rpm)	Number of layers	Calcination temperature (°C)
Film 1	1	2,500	5	700
Film 2	2	2,500	5	700
Film 3	2	5,000	5	900
Film 4	2	5,000	10	900

Fig. 1 - Thermal analysis of the dried gel: TG - thermogravimetric analysis, DTG - the derivative of the thermogravimetric analysis with respect to time and DTA - differential thermal analysis.
Analiza termică a gelului uscat: TG - analiza termogravimetrică, DTG - derivata analizei termogravimetrice în raport cu timpul şi DTA - analiza termică diferenţială.

indicates a weight loss of approximately 56 % over the entire temperature range. This weight loss can be divided in five stages, as follows: 27-150, 150-350, 350-500, 500-650 and 650-800 °C, all of them being associated with endothermic effects. Thus, the first weight loss is attributed to the evaporation of water and alcohols involved in the synthesis, the second to the dehydration of recrystallized hydrated nitrates, the third and forth to the decomposition of nitrate-type precursors, while the fifth to the decomposition of more stable species. The DTA curve also shows an exothermic effect with maximum at about 290 °C, which overlaps over the other effects and can be assigned to a possible combustion of the organic part. Since approximately 96 % of the gas generating components are eliminated up to 650 °C, it is obvious that the calcination temperature should exceed this value, a higher increase of this parameter having implications mainly on the crystallinity degree and particle size.

Fig. 2 shows the XRD patterns of the samples calcined at 700 or 900 °C. The lower temperature led to a vitroceramic mass composed of a glassy matrix and a family of merwinite ($Ca_3MgSi_2O_8$, $3CaO \cdot MgO \cdot 2SiO_2$, C_3MS_2) crystals with monoclinic structure (ICDD 00-074-0382); the vitreous phase is confirmed by the large bands that occur at low angles, while the crystalline one by the sharp peaks which were indexed with Miller indices. Going to the higher temperature, most of the diffraction maxima are typical of akermanite ($Ca_2MgSi_2O_7$, $2CaO \cdot MgO \cdot 2SiO_2$, C_2MS_2) phase with tetragonal symmetry (ICDD 00-083-1815); merwinite becomes the secondary phase in this case. Further, the average crystallite size was estimated by employing Scherrer equation: $D=K \cdot \lambda/(\beta \cdot cos\theta)$, where K is a dimensionless shape factor with a typical value of about 0.9, λ is the X-

ray wavelength (0.154 nm), β is the full width at half maximum value and θ is Bragg angle. Thus, the specimen calcined at 900 °C contains crystallites of akermanite with an average dimension of 41 nm, obtained through mediation on the first three most intense diffraction peaks.

Taking into consideration the main oxides (SiO_2, CaO and MgO) and their concentrations (38 %, 36 % and 18 %), the corresponding phase thermal equilibrium diagram reveals akermanite as primary crystalline phase in the case of a classic approach. However, since the applied preparation method is a non-conventional one, the phase composition evolution for the samples can be quite different. Moreover, the use of a crystalline substrate with hexagonal symmetry may have important implications on the nucleation and growth processes.

Marzban [23] obtained akermanite by mechanical activation and thermal treatment at 1100 °C, starting from SiO_2, CaO and MgO with molar ratio of 2:2:1, which is similar to the composition selected in this paper (2.1:2:1); the samples ball milled for 6 or 8 h contained a small amount of merwinite, while in the case of 10 h, pure akermanite phase was achieved. Mihailova *et al.* [24] also explored SiO_2–CaO–MgO system due to the good bioactivity and potential use as bone implants of the resulting ceramics; biphasic merwinite-akermanite bioceramics were achieved through the sol-gel method and a thermal treatment at 1300 °C.
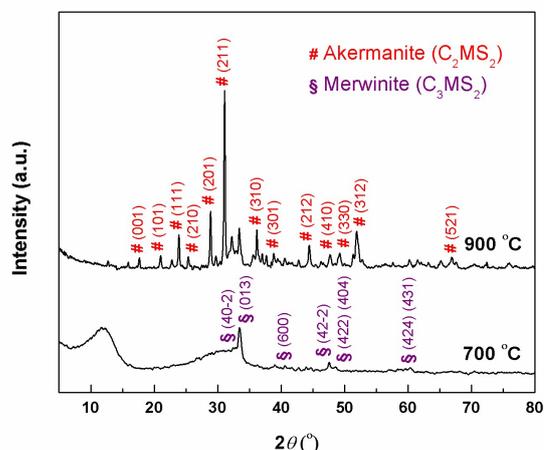

Fig. 2 - XRD patterns of the samples calcined at different temperatures. / *Analizele XRD ale probelor calcinate la diferite temperaturi.*

The deposition of thin films on the titanium plates was demonstrated through the FT-IR spectra recorded both for the neat substrate and covered ones, as it can be seen in Fig. 3. As opposed to the metallic substrate spectrum, which presents a slight and uniform increase in the investigated wavenumber range, the films spectra exhibit well-defined broad bands below 1000 cm^{-1}, attributed to the vibrations of the following bonds: Si-O, Ca-O and Mg-O [25].
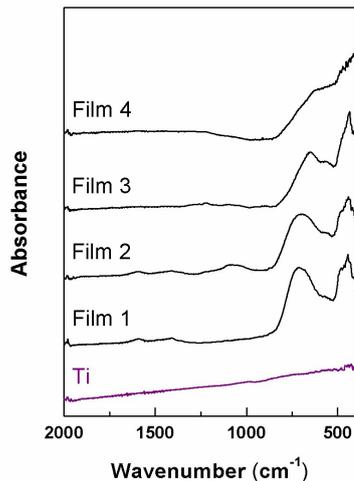
Fig. 3 - FT-IR spectra of the thin films deposited by spin coating and calcined at different temperatures. / *Spectrele FT-IR ale filmelor subţiri depuse prin centrifugare şi calcinate la diferite temperaturi.*

Figs. 4 and 5 highlight the surface morphology of the calcined thin films deposited by spin coating in different conditions. The samples thermally treated at 700 °C have a similar aspect at high magnification, with tightly packed grains that present sizes below 100 nm (Figs. 4b and d), but at low magnification, different micronic roughness can be observed (Figs. 4a and c). The difference between the two samples (Film 1 and Film 2) consists in the volume of the solution deposited on the substrate surface at the beginning of the procedure; it is obvious that a larger volume of precursor solution triggers a more accentuated roughness because of the changes occurred in the solution flow and solvent evaporation processes. Doubling the solution volume causes the growth of the layer thickness, as well as modified kinetics of

volatilization, with areas for which the evaporation rate is enhanced, leading to grooves in the texture, and areas with delayed evaporation, resulting in longitudinal hills crossing the surface.

A higher calcination temperature of 900 °C changes the microstructure of the films surface and favours the emergence of faceted grains with well-defined edges and corners, grown in a perfect joint that completely eliminates the material porosity (Figs. 5b and d). The grain average size is of approximately 1 μm for both samples and even the growth steps are clearly visible in the SEM images. Doubling the number of deposited layers (Fig. 5a as against Fig. 5c) has a similar effect as doubling the solution volume, namely an increase of roughness due to the fact that each layer copies and even amplifies the defects of the previous layer.

Another confirmation of the thin films deposition was provided by the EDX investigation, presented in Fig. 6. Both the qualitative and quantitative analyses available for Film 1 indicate the presence of all targeted elements on the surface of titanium substrate, but the concentrations are slightly modified in comparison with the designed values. This could be a consequence of local inhomogeneities associated to the intrinsic nature of a vitroceramic material.

The biological evaluation supposed the immersion of the coated substrates in SBF for 14 days, followed by their delicate washing with distilled water and drying. Fig. 7 exhibits the surface morphology after SBF soaking only for Film 1 and Film 2, since these are the only ones that promoted the formation of apatite phase as a result of ionic exchanges between the films and SBF. The new mineral layer grew either as a rough
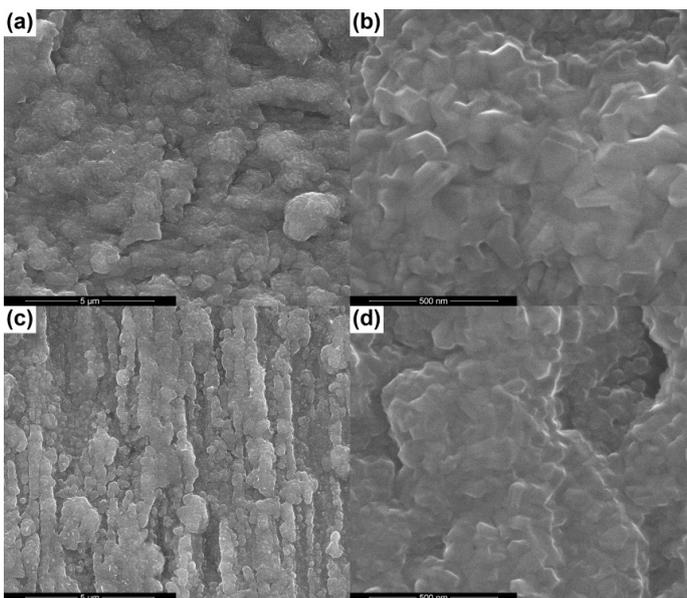

Fig. 4 - SEM images at different magnifications of the thin films deposited by spin coating and calcined at 700 °C: (a and b) Film 1 and (c and d) Film 2.
Imagini SEM la diferite măriri ale filmelor subţiri depuse prin centrifugare şi calcinate la 700 °C: (a şi b) Film 1 şi (c şi d) Film 2.
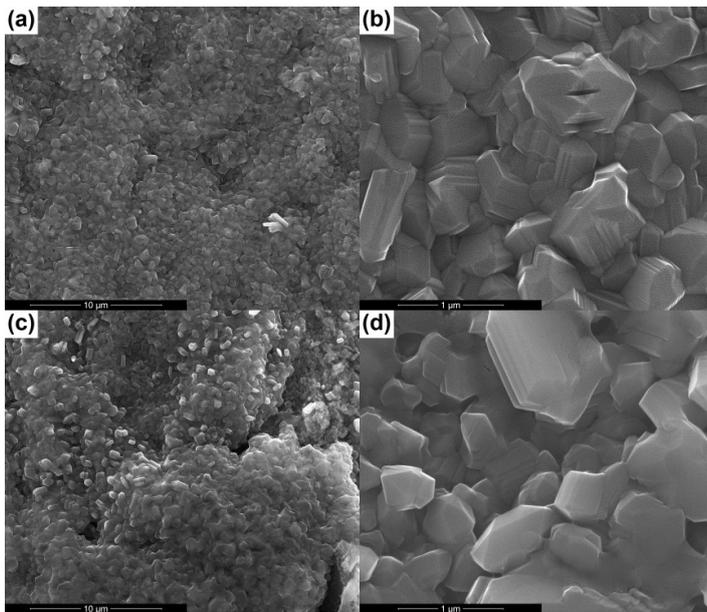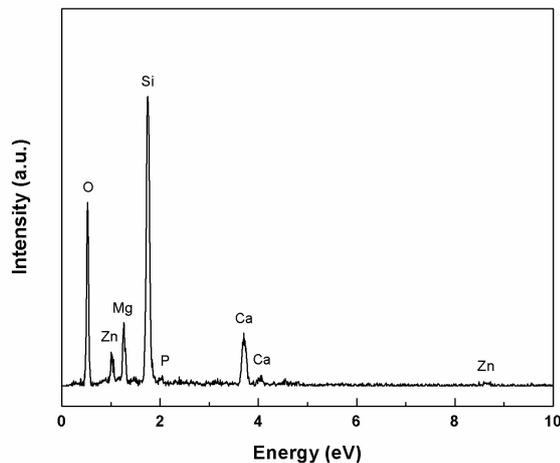
Fig. 5 - SEM images at different magnifications of the thin films deposited by spin coating and calcined at 900 °C: (a and b) Film 3 and (c and d) Film 4.
Imagini SEM la diferite măriri ale filmelor subţiri depuse prin centrifugare şi calcinate la 900 °C: (a şi b) Film 3 şi (c şi d) Film 4.

Element	Composition	
	Weight %	Atomic %
Si	28.07	20.57
P	0.81	0.54
Ca	9.41	4.83
Mg	6.41	5.43
Zn	2.26	0.71
F	1.53	1.66
O	51.52	66.27

Fig. 6 - EDX spectrum and composition of Film 1. / *Spectrul EDX şi compoziţia Filmului 1.*
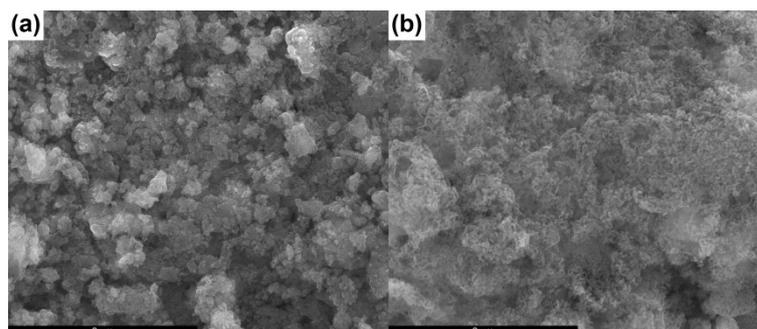

Fig. 7 - SEM images of the thin films after immersion in SBF for 14 days: (a) Film 1 and (b) Film 2.
Imagini SEM ale filmelor subţiri după imersare în SBF timp de 14 zile: (a) Film 1 şi (b) Film 2.

coating composed of particle agglomerates or as a fine network with laced appearance. Even though a correct compositional analysis of apatite is impossible to acquire because it contains the same elements as the films (Ca and P), its formation is not to be fought since the morphological features of the emerged structures are characteristic for apatite [13, 26].

The explanation for such behaviour is based on the porous texture generated by the sol-gel method and siloxane groups retention on the material surface thanks to the processing at a lower temperature (700 °C). All these features create appropriate sites for apatite nucleation and favourable conditions for biomaterial - cells interaction [27]. Moreover, the rigid crystalline structure of the samples calcined at 900 °C is not prone to ionic exchanges with the biological environment.

4. Conclusions

SiO_2–P_2O_5–CaO–MgO–ZnO–CaF_2 system was explored with the aim of producing bioactive layers suitable for the coverage of metallic implants employed in dentistry and orthopaedics. The sol-gel method was approached for ensuring a good purity and homogeneity, followed by spin coating, techniques that leads to uniform and thin films. The coatings calcined at 700 °C presented a vitroceramic structure, with merwinite as crystalline phase, and a good bioactivity when immersed in SBF for 14 days. In contrast, the films thermally treated at 900 °C were almost totally crystalline, with akermanite-type structure and lack of any biological response in SBF. A further optimization of the processing parameters could lead even to better results in terms of bioactivity and biocompatibility.

REFERENCES

1. S. Prasad, M. Ehrensberger, M. Prasad Gibson, H. Kim and E.A. Monaco Jr., Biomaterial properties of titanium in dentistry, Journal of Oral Biosciences, 2015, **57**, 192.
2. W. Wang and C.K. Poh, Titanium alloys in orthopaedics, in J. Sieniawski and W. Ziaja (Editors), Titanium alloys, IntechOpen, 2013, 1.
3. N.S. Manam, W.S.W. Harun, D.N.A. Shri, S.A.C. Ghani, T. Kurniawan, M.H. Ismail and M.H.I. Ibrahim, Study of corrosion in biocompatible metals for implants: A review, Journal of Alloys and Compounds, 2017, **701**, 698.
4. V. Sansone, D. Pagani and M. Melato, The effects on bone cells of metal ions released from orthopaedic implants. A review, Clinical Cases in Mineral and Bone Metabolism, 2013, **10**, 34.
5. S. Parithimarkalaignan and T.V. Padmanabhan, Osseointegration: An update, Journal of Indian Prosthodontist Society, 2013, **13**, 2.
6. M.M. Machado Lopez, J. Faure, M.I. Espitia Cabrera and M.E. Contreras Garcia, Structural characterization and electrochemical behavior of 45S5 bioglass coating on Ti6Al4V alloy for dental applications, Materials Science and Engineering B, 2016, **206**, 30.
7. A. Rodriguez-Contreras, Y. Garcia, J.M. Manero and E. Ruperez, Antibacterial PHAs coating for titanium implants, European Polymer Journal, 2017, **90**, 66.
8. G. Ciobanu and M. Harja, Cerium-doped hydroxyapatite/collagen coatings on titanium for bone implants, Ceramics International, 2018, https://doi.org/10.1016/j.ceramint.2018.07.290.
9. B.G.X. Zhang, D.E. Myers, G.G. Wallace, M. Brandt and P.F.M. Choong, Bioactive coatings for orthopaedic implants - Recent trends in development of implant coatings, International Journal of Molecular Sciences, 2014, **15**, 11878.
10. R. Family, M. Solati-Hashjin, S.N. Nik and A. Nemati, Surface modification for titanium implants by hydroxyapatite nanocomposite, Caspian Journal of Internal Medicine, 2012, **3**, 460.
11. G. Voicu, D. Miu, I. Dogaru, S.I. Jinga and C. Busuioc, Vitroceramic interface deposited on titanium substrate by pulsed laser deposition method, International Journal of Pharmaceutics, 2016, **510**, 449.
12. C. Busuioc, G. Voicu, I.D. Zuzu, D. Miu, C. Sima, F. Iordache and S.I. Jinga, Vitroceramic coatings deposited by laser ablation on Ti-Zr substrates for implantable medical applications with improved biocompatibility, Ceramics International, 2017, **43**, 5498.
13. G. Voicu, V.L. Ene, D.F. Sava, V.A. Surdu and C. Busuioc, Sol-gel derived vitroceramic materials for biomedical applications, Journal of Non-Crystalline Solids, 2016, **449**, 75.
14. S. Gnanam and V. Rajendran, Luminescence properties of EG-assisted SnO_2 nanoparticles by sol-gel process, Digest Journal of Nanomaterials and Biostructures, 2010, **5**, 699.
15. M. Cernea, Sol-gel processes with titanium precursors, Printech Publishing House, Bucharest, 2009.
16. D.E. Stan and D. Bojin, Adherent glass-ceramic thin layers with bioactive potential deposited by magnetron sputtering techniques, University POLITEHNICA of Bucharest Scientific Bulletin B, 2010, **72**, 187.
17. C. Busuioc, S.I. Jinga and E. Andronescu, Barium magnesium tantalate thin films obtained by sol-gel processing, Romanian Journal of Materials, 2012, **42**, 299.
18. S.L. Iconaru, E. Andronescu, C.S. Ciobanu, A.M. Prodan, P. le Coustumer and D Predoi, Biocompatible magnetic iron oxide nanoparticles doped dextran thin films produced by spin coating deposition solution, Digest Journal of Nanomaterials and Biostructures, 2012, **7**, 399.
19. D.P. Birnie, Spin coating technique, in M.A. Aegerter and M. Mennig (Editors), Sol-gel technologies for glass producers and users, Springer, Boston, Massachusetts, USA, 2004, 49.
20. M. Mehrjoo, J. Javadpour, M.A. Shokrgozar, M. Farokhi, S. Javadian and S. Bonakdar, Effect of magnesium substitution on structural and biological properties of synthetic hydroxyapatite powder, Materials Express, 2015, **5**, 41.
21. R.T. De Silva, M.M.M.G.P.G. Mantilaka, K.L. Goh, S.P. Ratnayake, G.A.J. Amaratunga and K.M. Nalin de Silva, Magnesium oxide nanoparticles reinforced electrospun alginate-based nanofibrous scaffolds with improved physical properties, International Journal of Biomaterials, 2017, **2017**, 1391298.
22. T. Kokubo, H. Kushitani, S. Sakka, T. Kitsugi and T. Yamamuro, Solutions able to reproduce in vivo surface-structure changes in bioactive glass-ceramic A-W, Journal of Biomedical Materials Research, 1990, **24**, 721.
23. K. Marzban, Preparation and characterization of nanostructure akermanite powder by mechanical activation method, Nanomedicine Research Journal, 2016, **1**, 79.
24. I.K. Mihailova, L. Radev, V.A. Aleksandrova, I.V. Colova, I.M.M. Salvado and M.H.V. Fernandes, Novel merwinite/akermanite ceramics: In vitro bioactivity, Bulgarian Chemical Communications, 2015, **47**, 253.
25. E.V. Kalinkina, A.M. Kalinkin, W. Forsling and V.N. Makarov, Sorption of atmospheric carbon dioxide and structural changes of Ca and Mg silicate minerals during grinding: II. Enstatite, akermanite and wollastonite, International Journal of Mineral Processing, 2001, **61**, 289.
26. R.G. Carrodeguas, E. Cordoba, A.H. De Aza, S. De Aza and P. Pena, Bone-like apatite-forming ability of $Ca_3(PO_4)_2$-$CaMg(SiO_3)_2$ ceramics in simulated body fluid, Key Engineering Materials, 2009, **396-398**, 103.
27. M. Laczka, K. Cholewa-Kowalska and A.M. Osyczka, Bioactivity and osteoinductivity of glasses and glassceramics and their material determinants, Ceramics International, 2016, **42**, 14313.

****